Pramana – J. Phys. (2019) 92:13
https://doi.org/10.1007/s12043-018-1674-2

Electromagnetically-induced transparency-like transmission characteristics of a waveguide coupled to a microsphere resonator

C Y ZHAO[1,2,*] and C M ZHANG[3]

[1]College of Science, Hangzhou Dianzi University, Zhejiang 310018, China
[2]State Key Laboratory of Quantum Optics and Quantum Optics Devices, Institute of Opto-Electronics, Shanxi University, Taiyuan 030006, China
[3]Nokia Solutions and Networks, Hangzhou 310053, China
*Corresponding author. E-mail: zchy49@hdu.edu.cn

MS received 31 October 2017; revised 17 May 2018; accepted 8 June 2018; published online 10 November 2018

Abstract. The limitation of traditional microring mode resonance, the microsphere confocal cavity is the best candidate for a low loss and controllable linewidth. Based on the transform matrix method, we investigate the waveguide coupled to a microsphere whispering-gallery mode (WGM) system. We find that the confocal cavity mode is completely different from the traditional ring cavity mode. The confocal cavity mode is excited in asymmetrical dual microsphere systems, and the spectrum of asymmetrical dual microsphere systems appear as an electromagnetically-induced transparency (EIT)-like profile, whereas the spectrum of symmetrical dual microsphere systems appears as Lorentz profile. The traditional ring cavity mode is excited in the symmetrical single microsphere system.

Keywords. Microsphere resonators; confocal mode; asymmetrical.

PACS Nos 42.79.–e; 42.79.Gn

1. Introduction

As we know, the coupled mode theory is used to study the performance of single- and double-microring resonators. We find that 2×2 linearly distributed coupler [1,2] is equivalent to a waveguide and single microring resonator [3]. The 3×3 linearly distributed coupler [1,2] is equivalent to a waveguide and dual microring resonators [4].

The limitation of traditional microring mode resonance, the whispering-gallery mode (WGM) microsphere confocal cavity is the best candidate for a low loss, high $Q = \nu/\Delta\nu$ factor and controllable linewidth $\Delta\nu$ [5]. The all-optical analogue to electromagnetically-induced transparency (EIT) based on coupled microsphere resonators is widely used in slow light, nonlinear optics and quantum information processing. A common way to couple light inside a microsphere is using evanescent coupling from a tapered fibre. The pump light is injected from the side and the ring mode is excited by a spherical ring standing wave [6,7]. The taper waist usually changes gradually from the fibre diameter to the minimum value at the centre of the taper and the evanescent field overlap can be controlled very easily by changing the coupling point between the taper and the microsphere. In 2000, Cai *et al* [6,8] studied a single spherical cavity. In 2014, Peng *et al* [9] reported the EIT effect in two WGM microtoroidal resonators. In 2015, we investigated the EIT effect in asymmetrical dual microring systems. The transmission spectrum changes from the EIT-like profile to the Lorentz profile. The EIT-like phenomenon originates from the interference between two Lorentz profiles [10]. If the pump light is injected from the front, when the incident angle is less than the critical angle, a concentric mode is excited by axial-oscillating standing wave [8,11]. In this paper, we shall adopt the axial-oscillating standing wave and investigate the EIT-like transmission of the waveguide coupled to asymmetrical dual microsphere systems with the linewidth effect.

The organisation of the paper is as follows: In §2, we give the theoretical background of a taper-microsphere resonator. In §3, the resonance linewidth of the taper-microsphere resonator will be obtained by the theoretical analysis and numerical calculation of the confocal mode. Section 4 is gives conclusion.

2. The microsphere resonator

An optical-fibre taper is coupled to a silica/microsphere WGM system. A WGM can be represented by an optical ray, trapped near the surface of the microsphere and trace a zig-zag path around the equatorial plane. The incident light pulses create a stress field, which can slightly deform the microsphere dimension, and the spherical cavity changes to the flat ellipsoid cavity. Based on the open-cavity theorem [12], the symmetric concentric spherical cavity with the radius of curvature $\rho(x_1, y_1; x_2, y_2) \approx l - (x_1^2 + y_1^2)/2l - (x_2^2 + y_2^2)/2l - (x_1x_2 + y_1y_2)/l$, where l is the mirror plane spacing and the stability parameter $g_1 = g_2 = -1$. In terms of the Fraunhofer approximation [13], the terms $x_1^2 + y_1^2$ and $x_2^2 + y_2^2$ can be negligible, and we have $\rho(x_1, y_1; x_2, y_2) \approx l - (x_1x_2 + y_1y_2)/l$. The symmetric confocal cavity is with the radius of curvature $\rho(x_1, y_1; x_2, y_2) \approx l - (x_1x_2 + y_1y_2)/l$ and the stability parameter $g_1 = g_2 = 0$. Thus, the concentric spherical cavity is different from the confocal cavity.

The vacuum wavelength $\lambda_0 = 1.55\,\mu$m, the diameter of silica/microsphere $d = 350\,\mu$m and the refractive index $n_s = 1.45$. Based on the Mie scattering theory [14], the scattering coefficient is

$$\begin{aligned} b_n(x,m) &= \frac{B_n(x,m)}{B_n(x,m) - \mathrm{i}D_n(x,m)}, \\ B_n(x,m) &= mJ_{n-(1/2)}(mx)J_{n+(1/2)}(x) \\ &\quad - J_{n+(1/2)}(mx)J_{n-(1/2)}(x), \\ D_n(x,m) &= mJ_{n-(1/2)}(mx)Y_{n+(1/2)}(x) \\ &\quad - J_{n+(1/2)}(mx)Y_{n-(1/2)}(x), \end{aligned} \tag{2.1}$$

where J_n and Y_n are the spherical Bessel functions, and $m = 1.45$ is the relative refractive index between the sphere and the surrounding environment (air). We can obtain the mode number by calculating the real part b_{nr} of the Mie scattering coefficient as a function of x (figure 1).

We can see from table 1 that the silica/microsphere-ring resonator with confocal cavity mode is the best available optical microresonator. The small mode volume leads to a strong light–matter coherent coupling.

In this configuration, the Hermit–Gaussian standing wave is injected into the fibre taper and energy is most efficiently coupled to the equatorial mode. The presence of an evanescent field tail at the microsphere boundary excites the WGMs inside the spherical microresonator. The solution of cavity modes of the confocal resonator in spherical coordinates is the Hermit–Gaussian beam [11]

$$\psi_{nm}(x,y,z) = N\frac{w_0}{w(z)}\mathrm{e}^{-\mathrm{i}\phi}H_n\left(\frac{\sqrt{2}x}{w(z)}\right)H_m\left(\frac{\sqrt{2}y}{w(z)}\right), \tag{2.2}$$

where the indices m and n determine the shape of the profile in x and y, respectively. N is the normalisation constant and w_0 is the spot size of the Hermit–Gaussian beam. The phase of the confocal cavity $\phi = \theta + (m + n + 1)\tan^{-1}(2\xi^2/\theta)$, $\theta = kz$, $\xi = z/w_0$, for $n = m = 0$, a Gaussian beam $\phi_{\min} = \theta$ is obtained. This mode $\psi_{00}(x, y, z)$ is called the fundamental mode. $H_n(\sqrt{2}x/w(z))$ and $H_m(\sqrt{2}y/w(z))$ are the Hermite polynomials.

3. The linewidth effect

We shall present the transmission performance of dual microsphere resonators with the linewidth effect in this section.

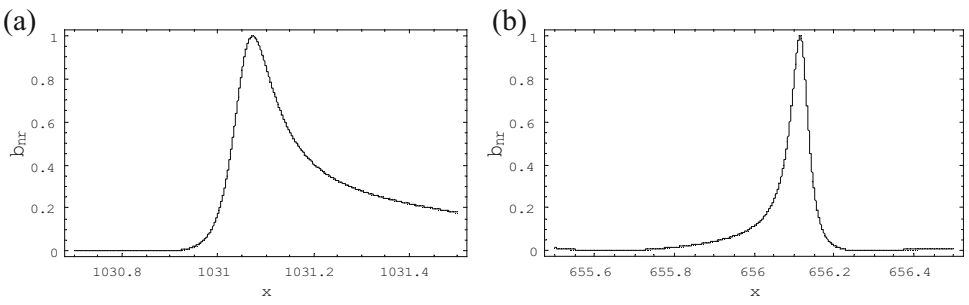

Figure 1. The mode number of (**a**) traditional microring cavity and (**b**) confocal cavity.

Table 1. Comparing microsphere with microring.

Material/resonator form	Mode	Mode number n	FWHM (nm)	Q factor
Polystyrene/microring	Traditional ring cavity	1031.1	145	3.5×10^5 [15]
Silica/microsphere	Confocal cavity	656.1	70	10^9 [16]

3.1 *The single microsphere system*

At critical coupling, the self-coupling coefficient $\tau = 0.9998$, the cross-coupling coefficient $\kappa = \sqrt{1-\tau^2}$ and the attenuation factor $\alpha = 0.9998$. Based on the coupled mode theory [2], we can obtain the transmission spectrum of figure 2b as follows:

$$T = \left|\frac{-\alpha+\tau e^{-i\vartheta}}{-\alpha\tau+e^{-i\vartheta}}\right|^2 = \left|\frac{(-\alpha+\tau e^{-i\vartheta})(-\alpha\tau^*+e^{i\vartheta})}{(-\alpha\tau+e^{-i\vartheta})(-\alpha\tau^*+e^{i\vartheta})}\right|^2$$

$$= \left|\frac{(-\alpha+\tau e^{-i\vartheta})(-\alpha\tau^*+e^{i\vartheta})}{(-\alpha\tau+e^{-i\vartheta})^2}\right|^2. \quad (3.1)$$

The phase factor $\vartheta = \theta$ for the ring mode [12] and the phase factor $\vartheta = \theta + i\zeta$ for the concentric mode [2], where ζ is the linewidth coefficient.

3.2 *Clockwise symmetrical dual microsphere systems*

The dual microsphere resonators are shown in figure 3a, and a waveguide coupled to the bottom of the microsphere 1, whereas the top of the microsphere 1 is far from the waveguide. Similarly, a waveguide coupled to the top of the microsphere 3, and the top of the microsphere 1 and the bottom of the microsphere 3 to be far apart from each other. The amplitude of the clockwise mode a_1 in microsphere 1 and the amplitude of the clockwise mode a_3 in microsphere 3 are given as follows:

$$a_1 = \alpha e^{i\theta} b_1, \quad a_3 = \alpha e^{i\theta} b_3. \quad (3.2)$$

Here, $\ln\alpha \leq 0$ represents the mode attenuation in one cycle. The attenuation is precisely determined by the linewidth effect. When $\ln\alpha > 0$, the mode gains in one cycle. $\ln\alpha$ is the gain coefficient.

When L is the circumference of the microsphere, we have the phase shift $\theta = \omega L/c = \omega\tau$, where c is the speed of light. The relation between the output power

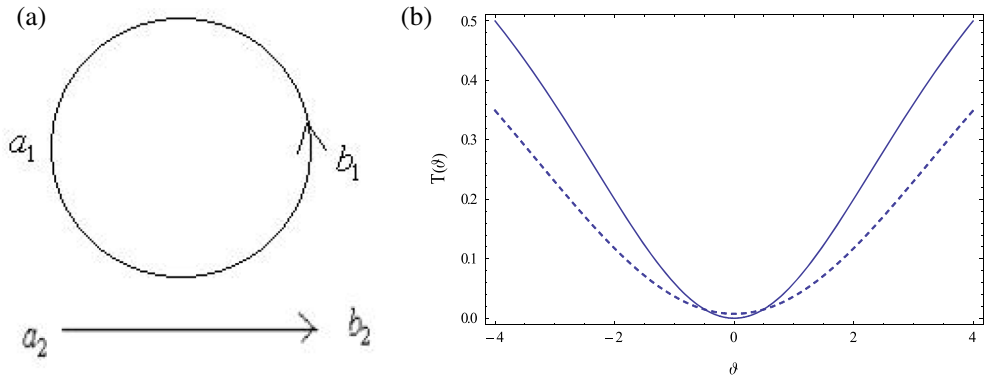

Figure 2. (**a**) Schematic diagram of the symmetrical single microsphere resonator. (**b**) The transmission spectrum T as a function of the phase factor ϑ for $\zeta = 0$ (ring mode, the solid line) and $\zeta = 0.5$ (concentric mode, the dashed line) with $\tau = \alpha = 0.9998$.

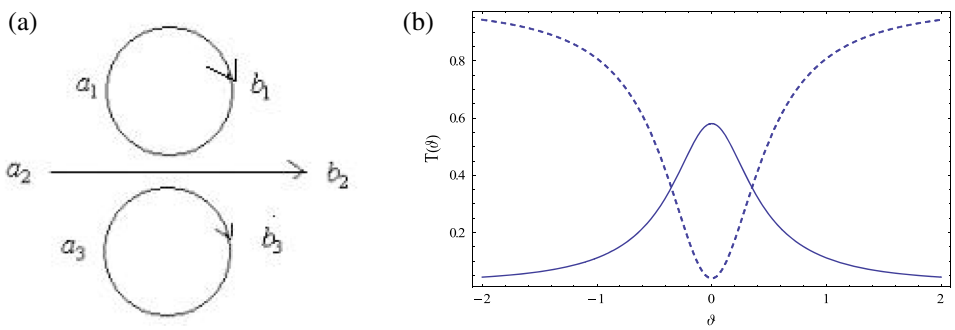

Figure 3. (**a**) Schematic diagram of the symmetrical dual microsphere resonators. (**b**) The transmission spectrum T as a function of the phase factor ϑ in asymmetrical dual microsphere systems (the solid line) and symmetrical dual microsphere systems (the dashed line) with $t = 0.8$, $\alpha_1 = 0.8t$, $\alpha_2 = 0.88t$.

$b(\tau)$ and the input power $a(\tau)$ can be expressed by the matrix relation [9]

$$\begin{pmatrix} b_1(\tau) \\ b_2(\tau) \\ b_3(\tau) \end{pmatrix} = \begin{pmatrix} \delta & k\ \gamma \\ -k & t\ k \\ \gamma & -k\ \delta \end{pmatrix} \begin{pmatrix} a_1(\tau) \\ a_2(\tau) \\ a_3(\tau) \end{pmatrix},$$

where

$$\delta = \frac{1}{2} + \frac{1}{2}t, \quad k = \frac{\mathrm{j}}{\sqrt{2}}\sqrt{1-t^2}, \quad \gamma = -\frac{1}{2} + \frac{1}{2}t,$$
$$t = \cos\left[\frac{\tau}{\sqrt{2}}\right]. \tag{3.3}$$

Based on [9], the transmission at the outport $T = |b_2/a_2|^2$, we also obtain Yariv's result $T = \left|(t\mathrm{e}^{-\mathrm{i}\theta} - \alpha)/(\mathrm{e}^{-\mathrm{i}\theta} - t\alpha)\right|^2$ for a single microsphere resonator [2]. As shown in figure 3b, we can see that the transmission spectrum of asymmetrical dual microsphere systems is sensitive to the attenuation factor α and the self-coupling coefficient t. The solid line corresponds to asymmetrical dual microsphere systems and the dashed line corresponds to symmetrical dual microsphere systems.

Considering the linewidth effect,

$$T = \left|t - \frac{\alpha(1-t^2)}{\mathrm{e}^{-\mathrm{i}\vartheta} - \alpha}\right|^2, \quad \vartheta = \theta + \mathrm{i}\zeta. \tag{3.4}$$

As shown in figure 4, the solid line corresponds to the asymmetrical dual microsphere systems, the narrow dashed line corresponds to the symmetrical dual microsphere systems and the wide dashed line corresponds to the symmetrical single microsphere system.

For non-critical coupling, the spectrum changes from the EIT-like shape to the Lorentz shape, whereas for critical coupling, the spectrum is unchanged and always retains the Lorentz shape.

3.3 *Clockwise asymmetrical dual microsphere systems*

As shown in figure 5a, a narrow linewidth tunable laser operated at a wavelength of $\lambda = 1550\,\mathrm{nm}$ is used to excite the system through the fibre import a_2. At near-resonance condition, for a 60.4-μm-diameter microsphere, the conference $L_1 = \pi \times 60.4\ \mu\mathrm{m} = 122\lambda$ and the phase shift $\theta_1 = \omega L_1/c$. At 67.5-μm-diameter microsphere, the conference $L_3 = \pi \times 67.5\ \mu\mathrm{m} = 137\lambda$

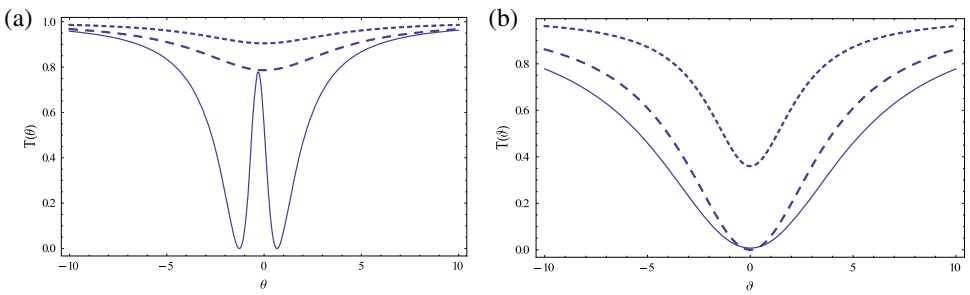

Figure 4. The transmission spectrum T as a function of phase factor θ in asymmetrical dual microsphere systems (the solid line), symmetrical dual microsphere systems (the narrow dashed line) and symmetrical single microsphere system (the wide dashed line): (**a**) $t = 0.9996$, $\alpha = 0.999975$ (non-critical coupling); (**b**) $\alpha = t = 0.9998$ (critical coupling).

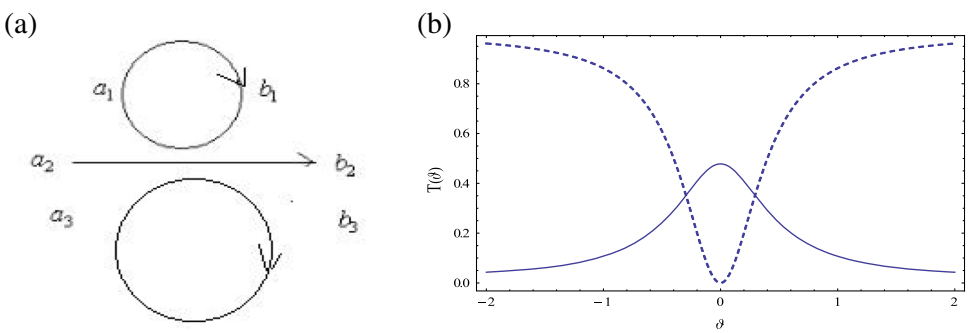

Figure 5. (**a**) Schematic diagram of the asymmetrical dual microsphere resonators. (**b**) The transmission spectrum T as a function of the phase factor θ in asymmetrical dual microsphere systems (the solid line), symmetrical dual microsphere systems (the dashed line) with $t = 0.8$, $\alpha_1 = 0.8t$, $\alpha_2 = 0.85t$.

and the phase shift $\theta_3 = \omega L_3/c$. The amplitude of the clockwise mode a_1 in microsphere 1 and the amplitude of the clockwise mode a_3 in microsphere 3 are given as follows:

$$a_1 = \alpha_1 e^{i\theta_1} b_1, \quad a_3 = \alpha_3 e^{i\theta_3} b_3. \tag{3.5}$$

The transmittance T becomes

$$T = \left| \frac{[1-(\delta-\gamma)\alpha_1 e^{i\theta_1}]\alpha_3 e^{i\theta_3} k}{1-\delta(\alpha_1 e^{i\theta_1}+\alpha_3 e^{i\theta_3})+(\delta^2-\gamma^2)\alpha_1\alpha_3 e^{i(\theta_1+\theta_3)}} \right|^2. \tag{3.6}$$

Comparing figures 3b and 5b, we find that the height of transmission of the asymmetrical dual microsphere systems is the same as that of the symmetrical dual microsphere systems, and the linewidths of the asymmetrical dual microsphere systems are narrower than that of the symmetrical dual microsphere systems.

3.4 *Counterclockwise symmetrical dual microsphere systems*

As shown in figure 6a, the amplitude of clockwise mode in microsphere 1 and the amplitude of the counterclockwise mode in microsphere 3, are

$$a_1 = \alpha e^{i\theta} b_1, \quad a_3 = \alpha e^{-i\theta} b_3. \tag{3.7}$$

Considering the linewidth effect, the transmission T becomes

$$T = \left| t - \alpha \frac{(\cos[\vartheta] - \alpha(2\cos^2[\vartheta]-1))(1-t^2)}{1-2\delta\alpha\cos[\vartheta]+\alpha^2 t} \right|^2. \tag{3.8}$$

The parameters are the same as in figure 7, and $\vartheta = 0.1$.

Comparing figure 7 with figure 3, in the case of non-critical coupling, the linewidth effect has a large influence on the transmission spectrum, whereas in the case of critical coupling, the position of the peak value of the curves decreases.

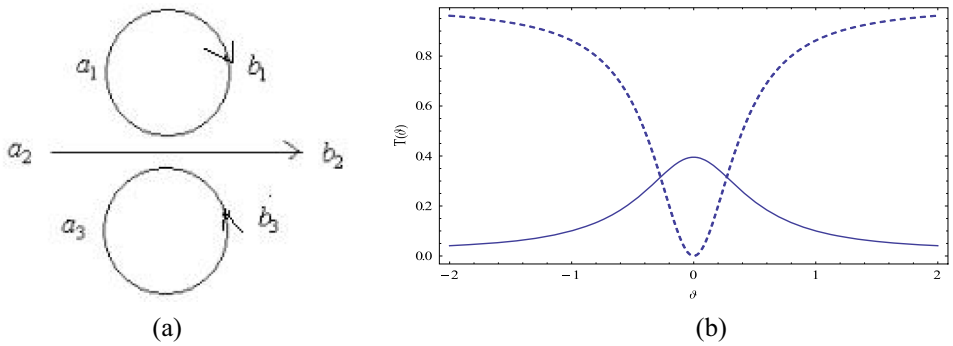

(a) (b)

Figure 6. (**a**) Schematic diagram of the symmetrical dual microsphere resonators. (**b**) The transmission spectrum T as a function of phase factor θ in asymmetrical dual microsphere systems (the solid line), symmetrical dual microsphere systems (the dashed line) with $t = 0.8$, $\alpha_1 = 0.8t$, $\alpha_2 = 0.82t$.

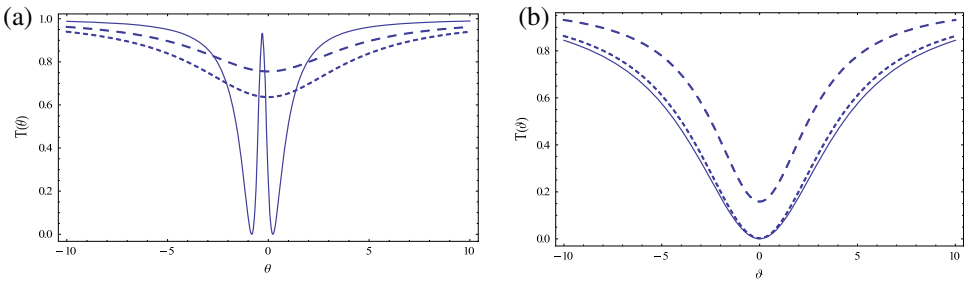

Figure 7. The transmission spectrum T as a function of phase factor ϑ with line-width effect in the asymmetrical dual microsphere systems (the solid line), symmetrical dual microsphere systems (the narrow dashed line) and symmetrical single microsphere system (the wide dashed line). (**a**) $t = 0.9996$, $\alpha = 0.99985$ (non-critical coupling); (**b**) $\alpha = t = 0.9998$ (critical coupling).

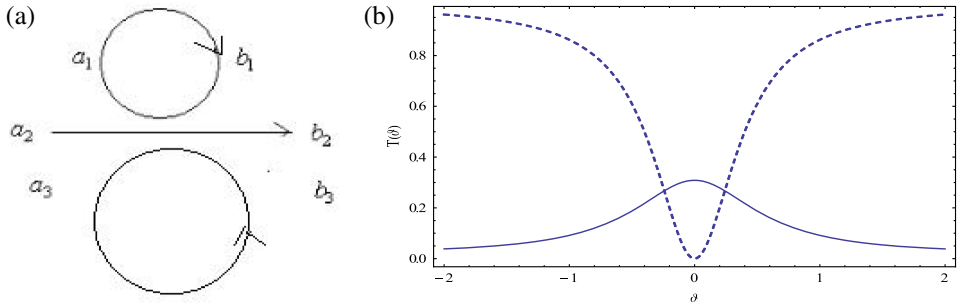

Figure 8. (**a**) Schematic diagram of the asymmetrical dual microsphere resonators. (**b**) The transmission spectrum T as a function of the phase factor ϑ with line-width effect in the asymmetrical dual microsphere systems (the solid line) and symmetrical dual microsphere systems (the narrow dashed line) with $t = 0.8$, $\alpha_1 = 0.8t$, $\alpha_2 = 0.78t$.

3.5 *Counterclockwise asymmetrical dual microsphere systems*

As shown in figure 8a, when $L_1 \neq L_2$, the amplitude of the clockwise mode a_1 in microsphere 1 and the amplitude of the counterclockwise mode a_3 in microsphere 3 are given as follows:

$$a_1 = \alpha_1 \mathrm{e}^{\mathrm{i}\theta_1} b_1, \quad a_3 = \alpha_3 \mathrm{e}^{-\mathrm{i}\theta_3} b_3. \tag{3.9}$$

The transmission T becomes

$$T = \left| t - \frac{1}{2} \frac{(1 - \alpha_1 \mathrm{e}^{\mathrm{i}\theta_1})\alpha_3 \mathrm{e}^{-\mathrm{i}\theta_3} + (1 - \alpha_3 \mathrm{e}^{-\mathrm{i}\theta_3})\alpha_1 \mathrm{e}^{\mathrm{i}\theta_1}}{(1 - \delta a_1 \mathrm{e}^{\mathrm{i}\theta_1})(1 - \delta a_3 \mathrm{e}^{-\mathrm{i}\theta_3}) - \gamma^2 \alpha_1 \alpha_3 \mathrm{e}^{\mathrm{i}(\theta_1 - \theta_3)}} (1 - t^2) \right|^2. \tag{3.10}$$

In the following, we investigate the transmission as a function of phase factors θ_1 and θ_3 with the linewidth effect. We take $\vartheta = 0.1$, $\mu = \theta_3/\theta_1$, $\zeta_1 = \theta_1 + \mathrm{i}\vartheta$, $\zeta_2 = \zeta_1 \mu$.

After considering the linewidth effect, we find that the height of transmission of asymmetrical dual microsphere systems is smaller than that of the symmetrical dual microsphere systems, and the linewidth of the asymmetrical dual microsphere systems is narrower than that of the symmetrical dual microsphere systems. Comparing figure 8 with figure 5, we find that the peak value decreases due to the linewidth effect.

4. Conclusion

In this paper, we investigate the influence of linewidth on the fibre taper coupled to dual microsphere systems with confocal cavity mode. Based on the transform matrix method, we compare a single microsphere system with dual microsphere systems. We investigate the transmission spectrum by controlling the self-coupling coefficient t, the attenuation factor α and the linewidth ζ. We find that the transmission spectrum of the asymmetrical dual microsphere systems has a large influence on the critical coupling situation, whereas the linewidth effect of the asymmetrical dual microsphere systems has a large influence on the non-critical coupling situation. In the case of critical coupling, the curves are nearly the same. We find that the transmission of the asymmetrical dual microsphere systems is narrower than that of the symmetrical situation. At the same time, the linewidth of the asymmetrical dual microsphere systems is narrower than that of the symmetrical situation.

Acknowledgements

This project was supported by the National Natural Science Foundation of China (Grant No. 11504074) and the State Key Laboratory of Quantum Optics and Quantum Optics Devices, Shan Xi University, Shan Xi, China (Grant No. KF201801).

References

[1] C Y Zhao, *Pramana – J. Phys.* **86**, 1343 (2016)
[2] Y C Meng, Q Z Guo, W H Tan and Z M Huang, *J. Opt. Soc. Am. A* **21**, 1518 (2004)
[3] A Yariv, *Electron. Lett.* **36**, 321 (2000)
[4] D D Smith and H Chang, *J. Mod. Opt.* **51**, 2503 (2004)
[5] M L Gorodetsky, A A Savchenkov and V S Ilchenko, *Opt. Lett.* **21**, 453 (1996)

[6] M Cai, O Painter and K J Vahala, *Phys. Rev. Lett.* **85**, 74 (2000)
[7] T Ioppolo, N Das and M V Otugen, *J. Appl. Phys.* **107**, 103105 (2010)
[8] M Cai, O Painter, K J Vahala and P C Sercel, *Opt. Lett.* **25**, 1430 (2000)
[9] B Peng, S K Özdemir, W J Chen, F Nori and L Yang, *Nat. Commun.* **5**, 5082 (2014)
[10] C Y Zhao and W H Tan, *J. Mod. Opt.* **62**, 313 (2015)
[11] C Y Zhao and F Ge, *J. Mod. Opt.* **61**, 435 (2014)
[12] Introduction of Solid-state Lasers Writing Group: *Introduction of solid-state lasers* (Shanghai People's Press, 1974)
[13] M Born and E Wolf, *Principles of optics*, 7th (expanded) edn (Cambridge University Press, Cambridge, 1999)
[14] S Schiller and R L Byer, *Opt. Lett.* **16**, 1138 (1991)
[15] T Ling, S L Chen and L J Guo, *Appl. Phys. Lett.* **98**, 204103 (2011)
[16] F Vollmer, S Arnold and D Keng, *Proc. Natl Acad. Sci. USA* **105**, 20701 (2008)